

Fig. 3 Critical dendrite tip concentration as a function of shrinkage parameter for quasisteady VDS.

in the iterations is not necessarily that given by the steady-state boundary condition, the term quasisteady is used to describe this approach.

The model was used with the property values and growth conditions of Tables 1 and 2, respectively.

Figure 2 presents selected neutral stability curves for various levels of shrinkage/expansion flow, and Fig. 3 illustrates the dependence of critical dendrite tip concentration on such flow. A shrinkage flow in the direction opposite that of the solidification direction tends to make the system more susceptible to convective breakdown, and an expansion flow tends to stabilize the system. There is a 14% difference between the stability criteria predicted for the case with shrinkage flow ( $\gamma = 0.295$ ) as opposed to the case with no shrinkage flow ( $\gamma = 0$ ).

### Conclusions

The effects of shrinkage flow are significant in determining the onset of convection during VDS of  $\text{NH}_4\text{Cl-H}_2\text{O}$ . Shrinkage flow was found to be destabilizing if in the direction opposite solidification, and stabilizing if in the direction of solidification. A difference of 14% was found between stability criteria for cases with and without shrinkage flow illustrating the importance of including the difference in phase densities in studies of convection during phase change processes.

### Acknowledgments

Funding for this work was provided through the NASA Office of Space Sciences and Applications under NAS8-37293. Rudy Ruff is the technical monitor.

### References

- <sup>1</sup>Neilson, D. G., and Incropera, F. P., "Unidirectional Solidification of a Binary Alloy and the Effects of Induced Fluid Motion," *International Journal of Heat and Mass Transfer*, Vol. 34, No. 7, 1991, pp. 1717-1732.
- <sup>2</sup>Beckermann, C., and Viskanta, R., "Double-Diffusive Convection During Dendritic Solidification of a Binary Mixture," *Physico-Chemical Hydrodynamics*, Vol. 10, No. 2, 1988, pp. 195-213.
- <sup>3</sup>Voller, V. R., Brent, A. D., and Prakash, C., "The Modelling of Heat, Mass, and Solute Transport in Solidification Systems," *International Journal of Heat and Mass Transfer*, Vol. 32, No. 9, 1989, pp. 1719-1731.
- <sup>4</sup>Poirier, D. R., Nandapurkar, P. J., Heinrich, J. C., and Felicelli, S., "Convection During Directional Solidification of Dendritic Alloys," *Materials Science Forum*, Vol. 50, Sept. 1988, pp. 65-78.
- <sup>5</sup>Prescott, P. J., and Incropera, F. P., "Numerical Simulation of a Solidifying Pb-Sn Alloy: The Effects of Cooling Rate on Thermosolutal Convection and Macrosegregation," *Metallurgical Transactions*, Vol. 22B, Aug. 1991, pp. 529-540.
- <sup>6</sup>Oldenburg, C. M., and Spera, F. J., "Numerical Modelling of Solidification and Convection in a Viscous Pure Binary Eutectic System,"

*International Journal of Heat and Mass Transfer*, Vol. 34, No. 8, 1991, pp. 2107-2121.

<sup>7</sup>Felicelli, S. D., Heinrich, J. C., and Poirier, D. A., "Simulation of Freckles During Vertical Solidification of Binary Alloys," *Metallurgical Transactions*, Vol. 22B, Dec. 1991, pp. 847-859.

<sup>8</sup>Hopkins, J. A., "Onset of Convection During Vertical Directional Dendritic Solidification and the Stabilizing Effect of the Two-Phase Region," Ph.D. Dissertation, Dept. of Mechanical Engineering, Univ. of Tennessee, Knoxville, TN, May 1992.

<sup>9</sup>Nandapurkar, P., Poirier, D. R., Heinrich, J. C., and Felicelli, S., "Thermosolutal Convection During Dendritic Solidification of Alloys: Part I. Linear Stability Analysis," *Metallurgical Transactions*, Vol. 20B, Oct. 1989, pp. 711-721.

<sup>10</sup>Worster, M. G., "Instabilities of the Liquid and Mushy Regions During Solidification of Alloys," *Journal of Fluid Mechanics*, Vol. 237, April 1992, pp. 649-669.

<sup>11</sup>Worster, M. G., "Natural Convection in a Mushy Layer," *Journal of Fluid Mechanics*, Vol. 224, March 1991, pp. 335-359.

<sup>12</sup>McCay, T. D., McCay, M. H., and Gray, P. A., "Experimental Observations of Convective Breakdown During Directional Solidification," *Physical Review Letters*, Vol. 62, No. 17, 1989, pp. 2060-2063.

<sup>13</sup>McCay, T. D., McCay, M. H., Lowry, S. A., and Smith, L. M., "Convective Instabilities During Directional Solidification," *Journal of Thermophysics and Heat Transfer*, Vol. 3, No. 3, 1989, pp. 345-350.

<sup>14</sup>Hopkins, J. A., McCay, T. D., and McCay, M. H., "Interferometric Measurements of a Dendritic Growth Front Solutal Diffusion Layer," AIAA Paper 91-1334, June 1991.

<sup>15</sup>Poirier, D. R., "Permeability for Flow of Interdendritic Liquid in Columnar-Dendritic Alloys," *Metallurgical Transactions*, Vol. 18B, March 1987, pp. 245-255.

## Evaluating the Temporal Accuracy of Inlet Normal Shock Propagation Simulations

Gerald C. Paynter\*

Boeing Commercial Airplane Group,  
Seattle, Washington 98124-2207

and

David W. Mayer†

Boeing Defense and Space Group,  
Seattle, Washington 98124-2207

### Introduction

ATMOSPHERIC disturbances encountered by a high-speed civil transport (HSCT) may induce an inlet unstart (expulsion of the normal shock) depending on the magnitude of the disturbance and the unstart tolerance of the inlet/engine combination. The NPARC<sup>1</sup> flow simulation software is being used to evaluate the unstart properties of a variety of inlet concepts, to support wind-tunnel tests aimed at evaluating inlet stability, and to support design of the inlet control system. Development of appropriate boundary conditions for unsteady Euler/Navier-Stokes inlet flow simulations has been under way for some time.<sup>2,3</sup> Now that appropriate boundary conditions are available for these simulations, the numerical time accuracy of the code for these tasks has become an important issue. Although NPARC can in theory be used to produce time-accurate

Received Oct. 3, 1994; revision received Feb. 24, 1995; accepted for publication March 6, 1995. Copyright © 1995 by the Boeing Company. Published by the American Institute of Aeronautics and Astronautics, Inc., with permission.

\*Boeing Associate Technical Fellow, Propulsion Research Staff, Engineering Division. Associate Fellow AIAA.

†Senior Specialist Engineer, Propulsion Technology Staff, Military Airplane Division. Senior Member AIAA.

inlet flow simulations, it was not originally intended for this purpose and validation of the code for unsteady flow has not yet been reported.

In an inlet unstart induced by a weak disturbance, the shock propagates forward (relative to the inlet geometry) at a velocity of only a few percent of the local speed of sound upstream of the shock. The purpose of the present study is to define a shock propagation problem with an analytic solution where the velocity and strength of a normal shock propagating upstream are similar to the velocity and strength of a normal shock in the throat of a mixed compression inlet during unstart. The use of the analytic solution to evaluate the accuracy of NPARC predictions with various solver and Courant–Friedrichs–Lewy (CFL) settings is then demonstrated. The analytic shock propagation problem is useful for investigating the effects of CFL number, grid stretching and density, and algorithm selection on the numerical accuracy of CFD solutions where a normal shock moves at low velocity.

### Test Problem and Analytic Solution

Shapiro<sup>4</sup> reports an analysis to compute the propagation velocity of a normal shock from the Mach number upstream and downstream

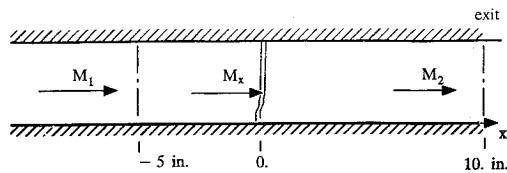


Fig. 1 Standing wave problem at  $t \leq 0$ .

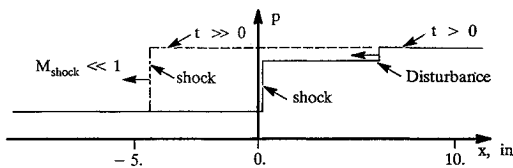


Fig. 2 Pressure distribution at  $t > 0$ .

of the shock. With reference to Fig. 1, the Mach numbers at states 1 and 2 are relative to a fixed frame of reference. The Mach number  $M_x$  is relative to a frame of reference moving with the shock.

From Shapiro, the following relation can be derived:

$$M_2 = \frac{-2M_x^2 + (\gamma - 1)M_1M_x + 2}{\sqrt{2(\gamma - 1)\gamma M_x^4 + [(\gamma + 1)^2 - 2(\gamma - 1)^2]M_x^2 - 2(\gamma - 1)}}$$

If  $M_1$  and  $M_2$  are assumed known, this equation can be solved for the Mach number of the flow relative to the shock wave. The Mach number of the shock relative to the geometry is  $M_x - M_1$ . The shock velocity in the test problem can be set equal to the shock velocity expected in an inlet through specification of  $M_1$ ,  $M_2$ , and the strength of the downstream disturbance  $M'_2$ .

### Results

The time accuracy of the various algorithm options in NPARC and the effect of step size on the accuracy of the solution were investigated by applying NPARC to the problem illustrated in Fig. 1. The values expected in a typical inlet wind-tunnel model with the normal shock in the design position were used to set the Mach number upstream of the shock, disturbance strength (change in Mach number at the right-hand boundary), distance from the right-hand boundary to the shock, and the distance from the shock to the left-hand boundary.

With  $M_1 = 1.3327$  and  $M_2 = 0.7699$ , the normal shock is stationary. At a reference  $\Delta t = 0.001265$  s, the Mach number at the exit plane was assumed to decrease by 5% to a value of 0.731405. The decrease in  $M_2$  causes a disturbance to propagate from the exit upstream to the shock and then the shock to propagate upstream as shown in Fig. 2. In the NPARC Euler simulations, constant inflow conditions were assumed, a slip wall was assumed at the upper and lower edges of the computational domain, and a constant Mach number outflow boundary condition with a step change at  $\Delta t = 0.001265$  s was assumed. At the subsonic outflow, the density and velocity were extrapolated from upstream and the static pressure adjusted to hold the Mach number at the desired value (the

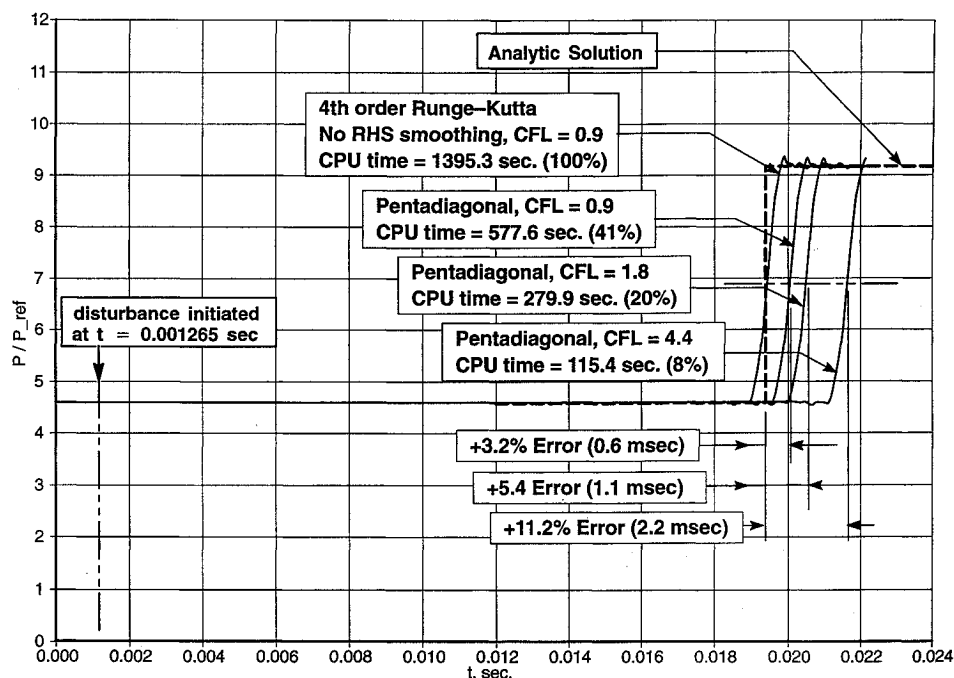


Fig. 3 Comparison of NPARC and analytic results at  $x = -5.0$  in.

time accuracy of NPARC outflow boundary conditions for unsteady flow simulations is still an issue).

Figure 3 shows the pressure as a function of time at a point 5.0 in. upstream of the initial normal shock location. Results are shown for the fourth-order Runge–Kutta solver without smoothing, CFL = 0.9, and the pentadiagonal solver with CFL = 0.9, 1.8, and 4.4. Results obtained with the Runge–Kutta solver with smoothing and CFL = 0.9 and 4.4 are not shown in Fig. 3 since the residual smoothing caused the wave speed to be underpredicted by approximately 50% for both CFL = 0.9 and 4.4.

It is apparent from Fig. 3 that the Runge–Kutta solver without smoothing and CFL = 0.9 gives excellent agreement with the analytic result. The pentadiagonal solver gives reasonable agreement for CFL numbers up to 4.4. The error in the predicted arrival time for the normal shock is 0.6 ms (3.2%) with CFL = 0.9 and 2.2 ms (11.2%) with CFL = 4.4. Note, however, that the calculations with the pentadiagonal solver are significantly less expensive with the required computer time reduced to between 8 and 41% of the computer time required for the Runge–Kutta solver. Also note that the shape of the pressure profile is nearly the same regardless of the solver or CFL setting.

### Conclusions

The following conclusions are drawn from this study.

1) The standing wave flow proposed for evaluation of numerical accuracy issues associated with inlet unstart simulations is similar to the unsteady flow in the throat of an inlet in an inlet unstart simulation. The disturbance strength in the standing wave analysis can be selected so that the velocity of the normal shock relative to a fixed frame of reference is almost identical to the velocity of the normal shock near the throat of an inlet during an inlet unstart. Since the shock propagation velocity for a shock tube is several orders of magnitude higher than that in the throat of an inlet for even a weak shock, the standing wave analysis is better for evaluating unsteady flow solver, grid, and time step options for inlet unstart simulations.

2) Residual smoothing causes the wave speed to be underpredicted (by about 50% for the conditions analyzed).

3) For the disturbance magnitudes anticipated for an HSCT inlet, the shape of the wave was preserved for all of the smoothing, solver, and CFL options investigated (i.e., fourth-order Runge–Kutta solver, pentadiagonal solver, and CFL = 0.9, 1.8, and 4.4).

4) Without residual smoothing, the fourth-order Runge–Kutta solver predicted a wave speed that was almost exactly equal to the analytic wave speed at a CFL = 0.9. For the same CFL number, the pentadiagonal solver was nearly as accurate. At CFL = 4.4, the wave speed predicted with the pentadiagonal solver was within 11.2% of the analytic. This would cause a lag in the wave arrival of about 2.2 ms for a typical inlet wind-tunnel model.

5) The CPU time required to achieve a solution with the pentadiagonal solver with CFL = 4.4 is only 8% of that required for Runge–Kutta solver with CFL = 0.9. A substantial saving in CPU time is possible if preliminary unsteady inlet simulations are done with the pentadiagonal solver with a CFL below 5. For more accuracy, the pentadiagonal solver can be used at a CFL less than 1. For best accuracy, the Runge–Kutta solver should be used at a CFL less than 1.

### References

- 1 Sirbaugh, J. R., Cooper, G. K., Smith, C. F., Jones, R. R., Towne, C. E., and Power, G. D., "A Users Guide to NPARC," NASA Lewis Research Center and Arnold Engineering and Development Center, NPARC Alliance Rept., Arnold Air Station, TN, Nov. 1994.
- 2 Mayer, D. W., and Paynter, G. C., "Boundary Conditions for Unsteady Supersonic Inlet Analyses," *AIAA Journal*, Vol. 32, No. 6, 1994, pp. 1200–1206.
- 3 Chung, J., "Numerical Simulation of a Mixed Compression Supersonic Inlet Flow," AIAA Paper 94-0583, Jan. 1994.
- 4 Shapiro, A. H., *The Dynamics and Thermodynamics of Compressible Fluid Flow*, Vol. 2, Ronald, New York, 1954, p. 1000.

## Unsteady Adaptive Wall Models for Wind-Tunnel Testing

Byeong-Hee Chang\* and Bongzoo Sung†

Korea Aerospace Research Institute,  
Taejon 305-333, Republic of Korea

and

Keun-Shik Chang‡

Korea Advanced Institute of Science and Technology,  
Taejon 305-701, Republic of Korea

### Introduction

THE adaptive wall test section technique has a distinct advantage over other devices for reduction of wall interference in wind-tunnel testing. For two-dimensional steady flows, the wall adaptation strategy has been well established and, to some extent, has been effectively applied to three-dimensional steady flows. For unsteady flow testing, wall adaptation would be conceptually perfect if the streamline could be obtained for a dynamic model in free flight for which the wind-tunnel test section wall is to be instantaneously adjusted. However, this idea has never been realized in wind-tunnel experiments. Fixed steady wall adaptation with an interference correction has been used instead in earlier unsteady flow experiments.<sup>1</sup> Since this approach was originally developed for pure subsonic or supersonic flows, it has limitations in application to transonic flows that contain a large supersonic flow region. There have also been difficulties for flows oscillating with large amplitude.<sup>1</sup> Instead, slotted or perforated walls have been widely put into practice with a reduced model size to lower the wall interference. In this study relatively simple unsteady adaptive two-dimensional wall models that can be used for the supercritical as well as subcritical oscillatory flows are proposed.

### Numerical Procedure

The finite volume method<sup>2</sup> is used for the Euler equations to numerically assess performance of the wall models for the wind-tunnel test section mounted with an oscillating airfoil. A resultant system of ordinary differential equations is integrated by a four-stage Runge–Kutta time-stepping scheme. The cell area changes with time when the airfoil and/or the wind-tunnel wall are in unsteady motion.

Unsteady flow around an oscillating airfoil in the wind-tunnel test section is treated by a composite grid system sketched in Fig. 1. The grid includes the buffer region I between the fixed H-mesh block and the oscillatory wall, and the buffer region II between the fixed H-mesh block and the O-mesh block embedding the airfoil that is under rigid oscillatory motion with the airfoil. The computational cells in these buffer regions undergo temporal deformation prescribed by spatial interpolation between the adjacent time-dependent boundary positions.

### Unsteady Adaptive Wall Models

Three adaptive wall models based on the streamline concept can be considered when the airfoil is in harmonic oscillation,  $\alpha = \alpha_m + \alpha_0 \sin \omega t$ . Here,  $\alpha$  is angle of attack and  $\omega$  is oscillation frequency. The simplest model will be the conventional adaptive wall model we call steady-streamline fixed adaptive wall

Received Nov. 1, 1994; revision received Feb. 4, 1995; accepted for publication Feb. 20, 1995. Copyright © 1995 by the American Institute of Aeronautics and Astronautics, Inc. All rights reserved.

\*Senior Researcher, Aerodynamics Department, 59, Oun-dong, Yusung-gu.

†Head, Aerodynamics Department, 59, Oun-dong, Yusung-gu. Member AIAA.

‡Professor, Department of Aerospace Engineering, 371-1, Kusung-dong, Yusung-gu. Member AIAA.